GSA Data Repository 2020183

Piazolo, S., et al., 2020, Melt-present shear zones enable intracontinental orogenesis: Geology, v. 48, https://doi.org/10.1130/G47126.1

Table DR3: Compilation of Palaeozoic geochronological data from the Arunta Region. Table DR3 compiles U-Pb, Sm-Nd, ^{40}Ar-^{39}Ar and K-Ar geochronological data from the Arunta region for the Palaeozoic period. The compilation used the following criteria: (1) ages must lie within the Alice Springs Orogeny timeframe (300–450/460 Ma; Buick et al., 2008), (2) ages must have error less than or equal to 20 Ma, and (3) ages were excluded when interpreted by the author(s) to reflect a cooling age.

References for Sources of data summarized in Table DR3 and shown in Figure 3

Ballèvre, M., Möller, A. and Hensen, B.J., 2000. Exhumation of the lower crust during crustal shortening: an Alice Springs (380 Ma) age for a prograde amphibolite facies shear zone in the Strangways Metamorphic Complex (central Australia). Journal of Metamorphic Geology, 18(6): 737-747.

Bendall, B., 2000. Mid-Palaeozoic shear zones in the Strangways Range: a record of intracratonic tectonism in the Arunta Inlier, central Australia. University of Adelaide, PhD thesis.

Bendall, B., Hand, M. and Foden, J., 1998. Sm-Nd evidence for mid-Palaeozoic regional amphibolite facies metamorphism in the Strangways Range, central Australia. Geological Society of Australia Abstracts, 49: 27.

Buick, I.S., Miller, J.A., Williams, I.S. and Cartwright, I., 2001. Ordovician high-grade metamorphism of a newly recognised late Neoproterozoic terrane in the northern Harts Range, central Australia. Journal of Metamorphic Geology, 19(4): 373-394.

Buick, I.S., Storkey, A. and Williams, I.S., 2008. Timing relationships between pegmatite emplacement, metamorphism and deformation during the intra-plate Alice Springs Orogeny, central Australia. Journal of Metamorphic Geology, 26(9): 915-936.

Cartwright, I., Buick, I. S., Foster, D. A., & Lambert, D. D. 1999. Alice Springs age shear zones from the southeastern Reynolds Range, central Australia. Australian Journal of Earth Sciences, 46(3): 355-363.

Cooper, J.A., Mortimer, G.E. and James, P.R., 1988. Rate of Arunta Inlier evolution at the eastern margin of the Entia Dome, central Australia. Precambrian Research, 40–41(0): 217-231.

Dunlap, W. J., Teyssier, C., McDougall, I., & Baldwin, S. 1991. Ages of deformation from K/Ar and 40Ar/39Ar dating of white micas. Geology, 19(12): 1213-1216.

Hand, M., Mawby, J., Kinny, P.D. and Foden, J., 1999. U-Pb ages from the Harts Range, central Australia: evidence for early Ordovician extension and constraints on Carboniferous metamorphism. Journal of the Geological Society, 156(4): 715-730.

Howlett, D., Hand, M., Raimondo, T., 2015. 120 Myr of episodic mid-crustal metamorphism and fluid-rock interaction during the Alice Springs Orogeny: the Strangways Range, central Australia. Poster session at the TIGeR conference, Curtin University, Perth, Western Australia.

Huston, D. L., Maas, R., Cross, A., Hussey, K. J., Mernagh, T. P., Fraser, G., & Champion, D. C. 2016. The Nolans Bore rare-earth element-phosphorus-uranium mineral system: geology, origin and post-depositional modifications. Mineralium Deposita, 51(6): 797-822.

Lavery, P., 2003. Petrological, stable isotope and geochronological constraints on the metamorphic fluid flow history of the Harts Ranges, central Australia. La Trobe University, PhD thesis.

Maidment, D.W., 2005. Palaeozoic high-grade metamorphism within the Centralian Superbasin, Harts Range region, central Australia. Australian National University, PhD thesis.

Maidment, D.W., Hand, M. and Williams, I.S., 2005. Tectonic cycles in the Strangways Metamorphic Complex, Arunta Inlier, central Australia: geochronological evidence for exhumation and basin formation between two high-grade metamorphic events. Australian Journal of Earth Sciences, 52(2): 205-215.

Maidment, D.W., Hand, M. and Williams, I.S., 2013. High grade metamorphism of sedimentary rocks during Palaeozoic rift basin formation in central Australia. Gondwana Research, 24(3–4): 865-885.

Mawby, J., Hand, M. and Foden, J., 1999. Sm–Nd evidence for high-grade Ordovician metamorphism in the Arunta Block, central Australia. Journal of Metamorphic Geology, 17(6): 653-668.

McLaren, S., Sandiford, M., Dunlap, W. J., Scrimgeour, I., Close, D., & Edgoose, C. 2009. Distribution of Palaeozoic reworking in the Western Arunta Region and northwestern

Amadeus Basin from 40Ar/39Ar thermochronology: implications for the evolution of intracratonic basins. Basin Research, 21(3): 315-334.

Möller, A., Armstrong, R., Hensen, B. and Williams, I., 1999a. Dating metamorphic events & deformation: Shrimp U–Pb zircon examples from the Strangways Metamorphic Complex, Arunta Inlier, Australia. European Union of Geosciences 10, Strasbourg, Journal of Conference Abstracts, 4: 711.

Möller, A., Williams, I.S., Jackson, S., and Hensen, B.J., 1999b. Palaeozoic deformation and mineral growth in the Strangways Metamorphic Complex: in-situ dating of zircon and monazite in a staurolite–corundum bearing shear zone. Geological Society of Australia Abstracts, 54: 71-72.

Mortimer, G. E., Cooper, J. A., & James, P. R. 1987. U/Pb and Rb/Sr geochronology and geological evolution of the Harts Range ruby mine area of the Arunta Inlier, central Australia. Lithos, 20(6): 445-467.

Raimondo, T., Clark, C., Hand, M., Cliff, J. and Harris, C., 2012. High-resolution geochemical record of fluid–rock interaction in a mid-crustal shear zone: a comparative study of major element and oxygen isotope transport in garnet. Journal of Metamorphic Geology, 30(3): 255-280.

Schoneveld, L., Spandler, C., & Hussey, K. 2015. Genesis of the central zone of the Nolans Bore rare earth element deposit, Northern Territory, Australia. Contributions to Mineralogy and Petrology, 170(2): 1-22.

Scrimgeour, I. and Raith, J.G., 2001. High-grade reworking of Proterozoic granulites during Ordovician intraplate transpression, eastern Arunta Inlier, central Australia. Geological Society, London, Special Publications, 184(1): 261-287.

Wade, B.P., Hand, M., Maidment, D.W., Close, D.F. and Scrimgeour, I.R., 2008. Origin of metasedimentary and igneous rocks from the Entia Dome, eastern Arunta region, central Australia: a U–Pb LA–ICPMS, SHRIMP and Sm–Nd isotope study. Australian Journal of Earth Sciences, 55(5): 703-719.

Supplementary Table DR1: Characteristics of compositionally and texturally distinct rock components (C1, C2, C3) identified in outcrop and thin section; data presented is derived from detailed field analysis and petrographic thin sections. For qualitative and quantitative thin section analyses observations were made on a suite of representative polished thin sections cut in the structural XY plane using a petrographic microscope, the Virtual Petrographic Microscope (Tetley and Daczko, 2014) and ImageJ 1.47v (Rasband, 1997-2015). Mineral abbreviations after Whitney and Evans (2010); S1 represents the shear foliation.

No	*Range of Bt content*	*Component geometry (shape and dimensions)*	*Mineral assemblage (area%)*	*Grain size*	*Microstructural characteristics*	*Nature of boundaries to other components*	*Additional Notes*
C1	< 5 %	- Continuous trains of apparent pinch-and-swell structures aligned parallel to S1; thickness 5-10 cm; individual swells are up to 1m long, but most commonly 20-40 cm; swell terminations are symmetrically thinning towards the tips; swells are up to 30 cm apart; commonly 2-5 mm seams dominated by Bt and minor Kfs + Qz are seen between swells; these are orientated parallel to S1; the geometry of the apparent "pinch and swell structures" closely resembles that of the "boudin-like intrusions" of Bons et al. (2004) (Fig. 2a); - Lenses with dominantly symmetrically thinning terminations with long axis aligned parallel to S1 (Fig. 2d); some occur as rootless folds with pinch-and-swell structures (Fig. 2b); thickness range: 0.5-10 cm; aspect ratio: 2-3	Bt (< 5%), Kfs (65-75%) Pl (5-12%) Qz (10-20%),	1-4 mm	- Kfs exhibits a small grain size range dominated by 2-3 mm, but may reach up to 4 mm; grains are commonly rectangular exhibiting crystal facets; - Kfs is microcline with cross-hatched crystal twinning (Fig. 2e), showing little undulose extinction and no core and mantle structures; - Pl grains (up to 2 mm) are rectangular exhibiting crystal facets; - Pl may in some cases form interstitial grains; - Pl and Kfs are commonly interlocked and without clear crystallographic or shape preferred orientation (Fig. 2e; DR2); - Qz grains are interstitial with frequent low dihedral angles and exhibit connectivity in three dimensions (i.e. interstitial grains that are spatially separate in 2D sections exhibit the same crystallographic orientation); grain may show very high aspect ratios of >8 and low dihedral angles at their terminations forming "films" (Fig. 2e; Vernon 2011); - Qz may show slight undulose extinction with some minor subgrain boundaries;	There are two boundary types towards Component 2 (note that one individual lens/swell may have different boundary types): a) 1-20 mm thick Bt selvedges (Fig. 2b, d,e); here Bt exhibits a strong preferred orientation parallel to the Component 1 (lens/swell) boundaries; in thick Bt selvedges individual rectangular Kfs grains or Kfs-Qz clusters may be present (Fig. 2d) b) no selvedges present (Fig. 2d); Towards Component 3 boundaries are undulatory following the shape of the lenses and apparent pinch and swell structures	Forms 10-20 vol.% of the shear zone (Fig. 2a) High frequency of lenses are seen in up to 50 cm wide, S1 parallel bands dominated by Component 2 (Fig. 2d).

					- Qz forms <0.1mm thick, elongate "fingers" with low dihedral angles towards the "invaded" Ksp (Fig. 2e); - Bt is only rarely kinked and shows no undulose extinction/crystal bending; - Bt within the bulk of the component exhibits no preferred shape or crystallographic orientation (Fig. 2e inset); - Some grain boundaries/interfaces are irregular (Fig. 2e)		
C2	5-25%	- occurs as continuous, S1 parallel bands over the whole outcrop (10-30 m); - thickness is constant within one continuous band and ranges from 0.1-1.20 m (Fig. 2a)	Bt (5-25%), Kfs (30-40%), Pl (15-20%), Qz (15-20%)	1 mm	- Bt is medium grained (~1 mm), aligned with S1 (Fig. 2b) forming the clear foliation, rarely kinked and lacks undulose extinction/crystal bending; - Kfs is microcline with cross-hatched crystal twinning (Fig. 2f) , showing little undulose extinction and no core and mantle structures; - Qz may show slight undulose extinction with some minor subgrain boundaries; - Qz grains are interstitial and exhibit connectivity in three dimensions; grain may show aspect ratios >8 forming "films" (Fig. 2f; Vernon, 2011) and frequent low dihedral angles (Fig. 2e); - Qz forms ~string of beads" textures (after Holness et al. 2011) characterized by arrays of 0.1-0.2mm, equidimensional quartz grain along Kfs-Kfs boundaries (Fig. 2f) - Some grain boundaries/interfaces are irregular, e.g. at the interfaces between Kfs and Qz (Fig. 2f);	There are two boundary types towards Component 1 (see above) a) 1-20 mm thick Bt selvedges (Fig. 2b, d-e); here Bt exhibits a strong preferred orientation parallel to the lens/swell boundaries; b) no selvedges present (Fig. 2d-e); Towards Component 3 the boundary is sharp, and subparallel to S1 but irregular along its length (Fig. 2c)	Forms main constituent of the shear zone (> 60 vol.%; Fig. 2a);
C3	>50%	- Occurs as continuous, S1 parallel bands over the whole outcrop (10-	Bt (> 50%), Kfs (<30 %),	Domi-natly	- Bt is medium grained (~1 mm), roughly aligned with S1, rarely kinked	Towards component 1 and 2 mostly sharp	Forms 15-25 vol.% of

		30 m); - thickness ranges from 0.5 cm to 1.5 m, however it is most commonly 10-30 cm (Fig. 2a); thickness is not always constant and may vary significantly (Fig. 2c); - in places this component may be seen as thin, mm- to cm- scale seams within component 1 and 2 (Fig. 2D; see above for details).	Pl (<5%) Qz (<30%), ± minor amounts (1-10%) of muscovite;, sillimanite, garnet, kyanite, staurolite, magnetite	1 mm	and lacks undulose extinction (Fig. 2g); - Qz grains form low apparent dihedral angles between two Bt grains and may form thin interstitial grains with aspect ratios > 8 (Fig. 2g); - In some cases Qz grains form elongate clusters aligned with S1; - Sillimanite/Staurolite/Muscovite, if present, are 0.2-0.5 mm in size and occur as elongate clusters with their elongation parallel to S1 (Fig. 2g); - Muscovite may also form an interstitial phase with similar shape characteristics as Qz (Fig. 2g); - Kfs (up to 3 mm) and Pl (up to 2 mm) grains are rectangular exhibiting crystal facets and occur interlocked with each other, these interlocked aggregates may form felsic, elongate clusters seen in S1 parallel trains (Fig. 2c); - Kfs is microcline with cross-hatched crystal twinning, showing little undulose extinction and no core and mantle structures.	boundaries at the scale of 1mm. Within Component 2: mm- to cm-thick seams of Component 3 may connect one felsic lens/swell (Component 1) to the other resulting in zones of Component 3 between individual lenses; these are subparallel to S1 (Fig. 2; to the right of inset box); here Component 3 often shows individual rectangular Kfs grains or elongate Kfs-Qz clusters (Fig. 2d)	the shear zone

References:

Bons, P. D., Druguet, E., Hamann, I., Carreras, J., & Passchier, C. W., 2004, Apparent boudinage in dykes: Journal of Structural Geology, v. *26*, p. 625-636.

Holness, M. B., Cesare, B., & Sawyer, E. W., 2011, Melted rocks under the microscope: Microstructures and their interpretation: Elements, v. 7, p. 247- 252.

Tetley, M. G., & Daczko, N. R., 2014, Virtual Petrographic Microscope: a multi-platform education and research software tool to analyse rock thin-sections: Australian Journal of Earth Sciences, v. 61, p. 631–637.

Rasband, W.S., 1997–2015, ImageJ: U. S. National Institutes of Health. Bethesda, MD, USA. Available at: http://imagej.nih.gov/ij/.

Whitney, D. L., & Evans, B. W., 2010, Abbreviations for names of rock-forming minerals: American Mineralogist, v. 95, p. 185–187.

Vernon, R. H., 2011, Microstructures of melt-bearing regional metamorphic rocks: Geological Society of America Memoirs, v. 207, p. 1–11.

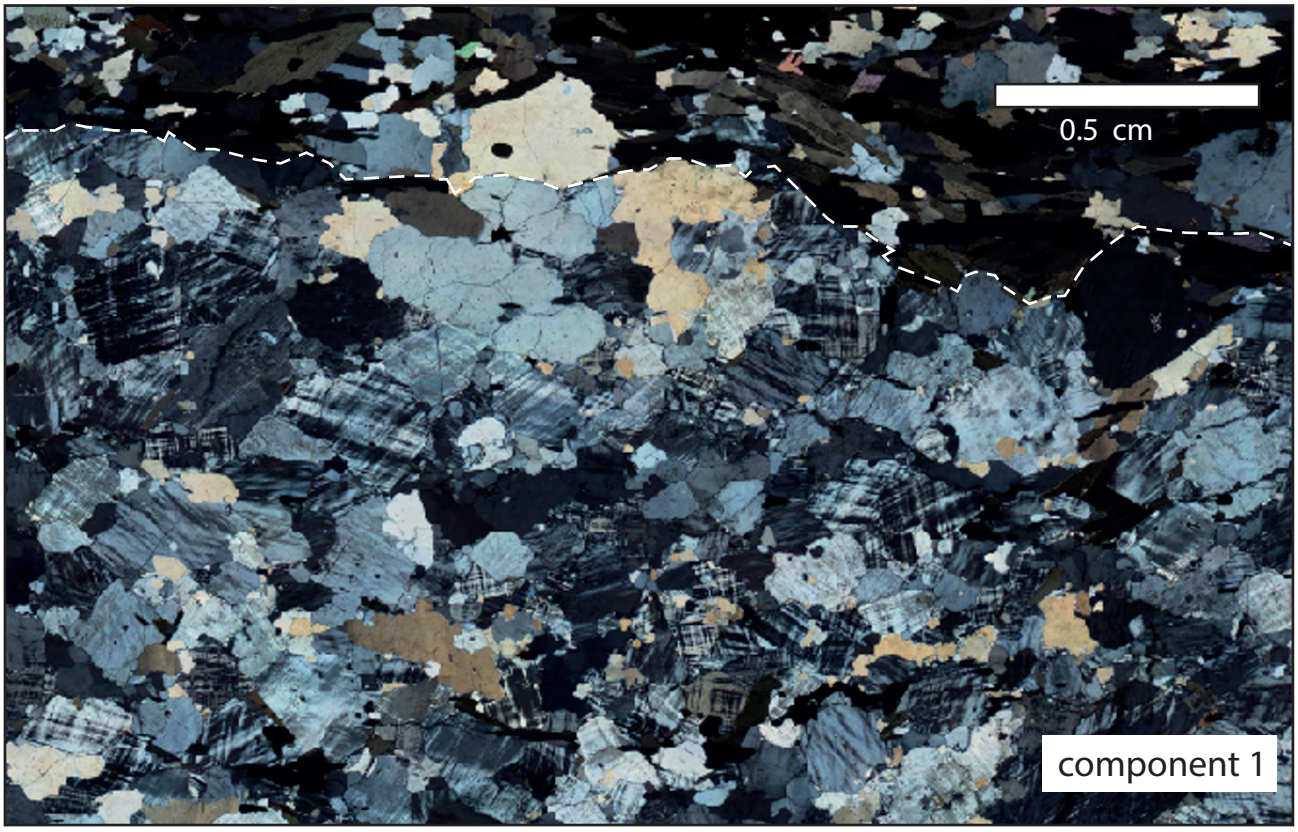

Supplemental Figure DR2:
Photomicrograph depicting an overview of component 1 which does not show any clear crystallographic or shape preferred orientation; note boundary between compnent 1 and surrounding (white stippled line) which is characterized by high abundance of biotite.